Direct Observation of Atom-Ion Nonequilibrium Sympathetic Cooling

Ziv Meir,* Meirav Pinkas, Tomas Sikorsky, Ruti Ben-shlomi, Nitzan Akerman, and Roee Ozeri
Department of Physics of Complex Systems, Weizmann Institute of Science, Rehovot 7610001, Israel

(Received 6 February 2018; published 2 August 2018)

Sympathetic cooling is the process of energy exchange between a system and a colder bath. We investigate this fundamental process in an atom-ion experiment where the system is composed of a single ion trapped in a radio-frequency Paul trap and prepared in a classical oscillatory motion with total energy of ∼200 K, and the bath is an ultracold cloud of atoms at μK temperature. We directly observe the sympathetic cooling dynamics with single-shot energy measurements during one to several collisions in two distinct regimes. In one, collisions predominantly cool the system with very efficient momentum transfer leading to cooling in only a few collisions. In the other, collisions can both cool and heat the system due to nonequilibrium dynamics in the presence of the ion trap's oscillating electric fields. While the bulk of our observations agree well with a molecular-dynamics simulation of hard-sphere (Langevin) collisions, a measurement of the scattering angle distribution reveals forward-scattering (glancing) collisions which are beyond the Langevin model. This work paves the way for further nonequilibrium and collision dynamics studies using the well-controlled atom-ion system.

DOI: 10.1103/PhysRevLett.121.053402

Sympathetic cooling is a key paradigm in physics of ultracold atoms and ions. With ions, sympathetic cooling is used to cool ionic species that lack laser-cooling transitions [1] and molecules [2–4] for the purpose of creating new time standards [5], testing fundamental physics theories [6,7], and performing low-temperature quantum-controlled chemistry with single particle resolution [8–10]. With ultracold neutral atoms, sympathetic cooling is used to achieve degeneracy in species with a small [11] or vanishing collision cross section such as low-temperature fermions [12]. Recently, sympathetic cooling with atoms was extended to cool macroscopic membranes [13].

Experimental systems overlapping ultracold atoms and ions are an excellent resource for studying not only sympathetic cooling [14–16] but also nonequilibrium dynamics [17,18]. The absence of equilibria emanates from the oscillating electric fields used to trap the charged ions [19]. These fields couple to the ion's motion during collisions [20] and can lead to both heating and cooling. The nonequilibrium dynamics results in a power-law distribution of ion energies [21–26] which was observed experimentally using narrow linewidth spectroscopy [18]. In that work, the ion's energy distribution was inferred from a steady-state Tsallis function fit to a mean signal of many experimental realizations. Here, we study the non-steady-state regime following single to few collisions and with direct ion energy measurements in each experimental realization, thus, using no *a priori* assumptions on the ion's energy distribution.

We use a newly developed thermometry technique [27] which is similar to Doppler-cooling thermometry (DCT) [28,29]; however, it utilizes different analytic tools and is suited for a different energy regime. DCT is used to extract the temperature of the ion assuming an underlying energy distribution and requires extensive averaging due to photon shot noise. In the new method, single-shot DCT (SSDCT), we extract the energy of the ion from each experimental realization, without averaging, leading to the direct reconstruction of its energy distribution with no underlying assumptions. The method relies on detecting the cooling time which is independently assigned for every repetition of the experiment. This method is also capable of identifying the spatial mode of ion motion with good statistical significance, an ability we exploit to measure the distribution of scattering angles.

We performed two distinct experiments. In both experiments, we prepared a single ion in a classical oscillatory state of ∼200 K mean and few K width of the energy distribution. This distribution resembles the motion of a classical harmonic oscillator. In the first experiment, we prepare the motion along the ion-trap axial mode, and we overlap the atoms with the trap center. In the second experiment, we prepare the motion in the radial mode, and we offset the atoms 20 μm above the trap center [see Fig. 1(a)]. In symmetric linear Paul traps, there are no oscillating electric fields along the trap axial axis such that collisions along this axis only cool the ion. Moreover, the atomic cloud finite size in the radial direction (5 μm) introduces an energy cutoff for the steady-state energy distribution tail of a few K [24,30] which allows the observation of nearly equilibrium dynamics in this inherently nonequilibrium system. In the second experiment, the ion is excited radially and samples trap regions with high-amplitude oscillating fields. Collisions with atoms in the

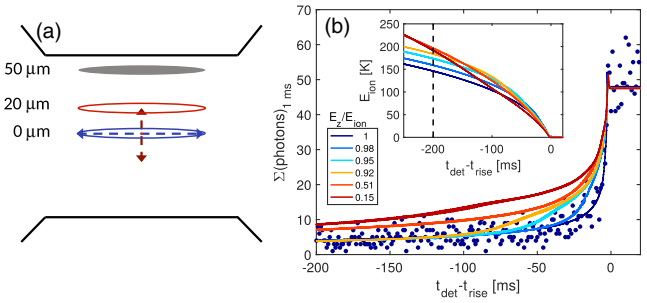

FIG. 1. (a) Two experimental configurations. Ellipses indicate the sizes and positions of the atomic cloud with respect to the ion-trap center. Gray is the initial position before interaction; blue (red) is the position in the axial (radial) equilibrium (nonequilibrium) experiment. Dashed arrows indicate the ion's initial motion amplitude in each of the experiments. Arrows and ellipses are to scale. The ion-trap axial axis (black lines, not to scale) coincides with the atom-trap long axis. (b) Single-shot Doppler-cooling thermometry. Dots are the measured fluorescence signal of an ion prepared solely in the trap's axial mode. Lines are the results of ion-fluorescence numerical calculations for different initial axial to total energy ratios (legend). Inset is the total ion's energy for the different numerical calculations. Dashed line indicates the ion's total energy for cooling time of 200 ms for the different calculations. In all graphs, zero time indicates the onset of reaching the Doppler temperature.

presence of these fields lead to nonequilibrium effects. Since the electric field amplitude in an ion Paul trap increases linearly with the radial distance from the trap center, we displace the atoms radially to allow for collisions in regions of high-amplitude fields.

Our experimental apparatus is described in detail in Ref. [26]. Briefly, we prepare an ultracold atomic sample (5 μK) consisting of ~7500 atoms in a crossed optical dipole trap, 50 μm above the trap center [Fig. 1(a)]. The ion is Doppler cooled and micromotion compensated at the trap center. We then excite the ion to an oscillatory state of motion using a short oscillating electric pulse close to resonance with the axial (or radial) mode frequency. This results in a narrow Gaussian distribution of energies [27]. Then, we move the atoms to overlap the ion. We scan the interaction time [31] and observe the effect of single to few collisions on the ion's energy distribution. We calculate a 0.7 kHz Langevin-collision rate [31]. To stop the interaction, we shut off the atom's dipole trap beams which leads to a fast decrease of the atomic density and halts atom-ion collisions. We then use the SSDCT to detect the ion energy and mode of motion for the specific experimental instance. This method (SSDCT) is described in detail in Ref. [27] and will only be briefly discussed in the following.

In SSDCT, we detect the ion's fluorescence during the course of Doppler cooling [blue dots in Fig. 1(b)]. At the cooling initial stage, the ion's fluorescence is low due to the large Doppler shifts associated with the ion's oscillatory motion. The photon-scattering level remains low for hundreds of ms until the Doppler shifts become comparable with the cooling transition linewidth. At this point, a sharp rise of the fluorescence signal indicates the last stage of cooling where the ion reaches the Doppler temperature limit. From a numerical calculation of the ion's trajectory in the presence of the cooling light, we determine the ion's scattering rate dynamics and compare it to the experimental measured fluorescence.

We repeat the numerical calculation for different energy partitions between the axial and radial modes of the ion motion. The results of these numerical calculations are shown in Fig. 1(b). We see that the initial partition of energy between the trap modes changes the fluorescence dynamics significantly. For energy distribution purely in the axial mode of the trap [dark blue line in Fig. 1(b)], the initial fluorescence level (high ion's energy) is low compared to the initial fluorescence level in the case of energy distributed considerably also in the radial modes (redder lines). Moreover, the fluorescence rise to the Doppler level at the last cooling stage is much sharper for the axially distributed energy. Both effects are caused by broadening of the spectrum due to micromotion sidebands [29,32]. The inset of Fig. 1(b) shows the evolution of the ion's total energy during the process of cooling. We see that the initial mode partition of energy also changes the cooling time. For an ion prepared in the axial mode of the trap (dark blue lines), the cooling time is longer compared to the more radially populated cases (redder lines). This effect is also attributed to the increased scattering due to micromotion and to the cooling lasers and trap geometry. The evolution of the energy in the different modes of the trap is given in Ref. [31].

We perform a likelihood ratio test (LRT) for the fluorescence curve of each single-shot experimental repetition with all the calculated numerical fluorescence trajectories and choose the one with the maximal likelihood value [27,31]. We use this numerical calculation to extract the ion's energy for the specific experimental instance and repeat the procedure for all other instances. We performed a stochastic numerical simulation to analyze the LRT method. The type I errors for assigning a wrong simulation to a trajectory are less than 1% when the cooling trajectory is longer than 100 ms [31].

The results of the experiment in which the ion motion is prepared along the axial mode and the atoms overlap the trap center are shown in Figs. 2(a)–2(f). The measured initial ion energy histogram before it collides with the atoms is shown in Fig. 2(a). The ion is in an oscillatory state with mean energy of 183.7 K. The Gaussian distribution width of 2.3 K is either due to imperfect initialization or inaccuracies in the energy measurement owing to fluctuations in the parameters of the cooling beams. The narrow distribution sets an upper limit for the SSDCT stability of ~1%. The accuracy of this method was estimated to be on the level of 5% in Ref. [27]. The LRT identified 98.4% of

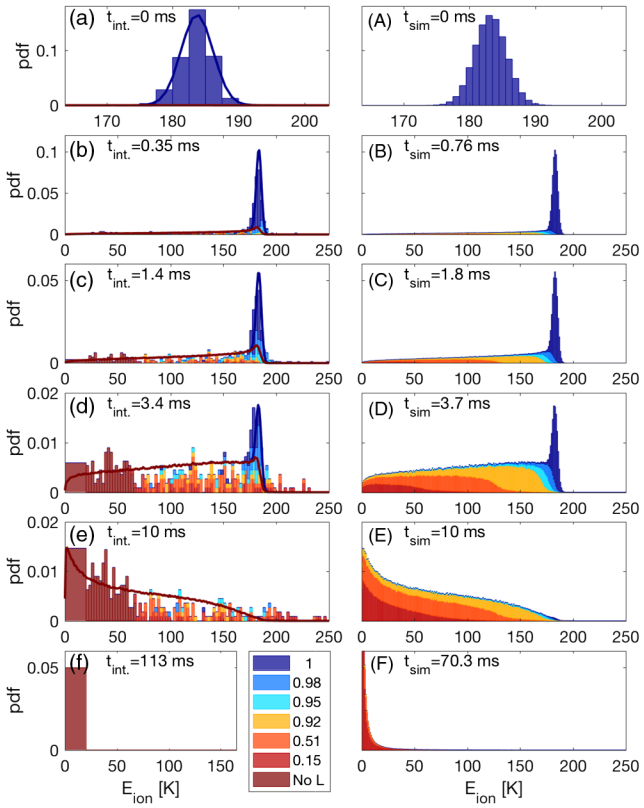

FIG. 2. Sympathetic cooling. (a)–(f) Experimentally measured energy histograms of the ion's total energy for different interaction times, t_{int} [31]. The color of the bars indicates the axial energy to total energy ratio of the ion according to the LRT analysis (see legend). The color code is the same as in Fig. 1(b). The dark red bars are cold events with cooling times less than 50 ms for which the LRT cannot determine the mode distribution [31]; however, the SSDCT can determine the energy. We use the steady-state energy distribution ($E_z/E_{\mathrm{ion}} = 0.15$) for these events. The lines are results of MD simulation which takes into account only Langevin collisions which are also presented in the right column. In the left column, the red line separates the simulation events with no collisions (above) and simulation events with one or more collisions (below). (A)–(F) MD-simulation energy histograms. The color of the bars indicates the axial energy to total energy ratio in the simulation binned according to the available numerical simulations. Simulation times t_{sim} are chosen to match the measured mean energy in the experiment.

the energies of the experimental events to distribute solely in the axial mode (dark blue) which sets an upper bound of 1.6% for the type II error for assigning a collision to no-collision event.

As the ion starts colliding with the atoms [Figs. 2(b)–2(e)], the energy histogram develops a tail of low energies, and the initial narrow Gaussian distribution depletes. This is a direct observation of sympathetic cooling in which a collision with essentially a zero-energy atom can take away all the energy of the ion (we use ^{87}Rb atoms and a $^{88}Sr^{+}$ ion with nearly equal masses). We also see that the mode of the collided events is no longer solely in the axial direction but contains a

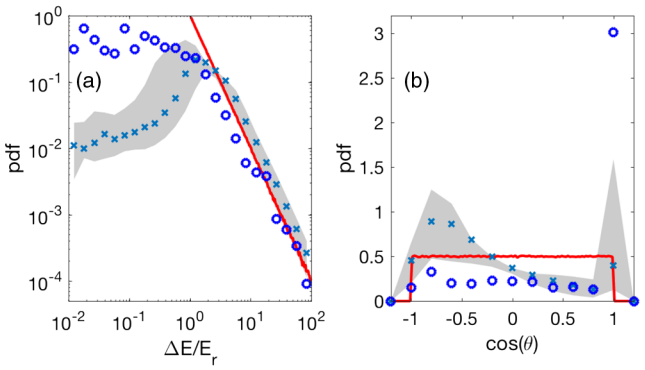

FIG. 3. Scattering angle distribution. Histograms of the energy difference divided by the radial energy after a collision (a) and the cosine of the scattering angle (b). Red lines are the theoretical prediction of Langevin scattering. Blue x's are an analysis of MD-simulation results [Figs. 2(A)–2(D)]. The analysis takes into account experimental limitations which modify the distributions. Gray areas reflect the uncertainty regions of the simulation analysis due to experimental limitations. The simulation treats only Langevin collisions [31]. Blue circles are calculated from the experimental data of Figs. 2(a)–2(d).

substantial fraction of energy in the radial direction as well (the color of the bars indicates the fraction of radial energy). This is a direct observation of the collision scattering angle for which a quantitative analysis is given in Fig. 3. We observe a small excess of collisions which result in energies above the ion's initial energy. These seemingly non-energy-conserving events are probably due to overestimation of the ion's energy for large scattering angles [see Fig. 1(b) inset].

We perform a molecular-dynamics (MD) simulation [22] to extract the ion energy and energy mode distribution. We use the experimentally measured initial energy distribution [Fig. 2(a)] as the initial conditions in the simulation [Fig. 2(A)]. The simulated energy histograms are shown in Figs. 2(B)–2(F) together with the distinction between the different energy partitions between modes of motion (color). We add the simulation results also to the experimental data figures [Figs. 2(a)–2(f) solid lines]. Here, the red lines separate the events which have undergone a Langevin collision and events which did not. In Figs. 2(c) and 2(d), we see a small excess of experimentally detected events in which motion was detected to be at a small angle to the longitudinal direction (light blue) compared to the MD-simulation predictions (red line). This observation indicates that our thermometry method is sensitive to glancing collisions which are not taken into account in the simulation.

To study this effect further, we perform a quantitative analysis of the scattering angle distribution shown in Fig. 3. For the case of a free ion moving at a constant velocity colliding with a zero-energy atom, the energy transferred to the atom ΔE and the ion deflection angle θ are correlated. We can neglect the ion's trapping harmonic potential in the collision analysis since the collision is instantaneous as compared with the ion harmonic trap frequency. However,

due to the harmonic potential, we can only experimentally measure the total energy (kinetic and potential) of the ion after a collision occurs and not its velocity. We, therefore, use an observable $\Delta E/E_r$, which is independent of the velocity of the ion prior to the collision [31],

$$\cos(\theta) = \left(\frac{m}{M} - \left|\frac{\Delta E}{E_r} - \frac{m}{M}\right|\right) \Big/ \frac{\Delta E}{E_r}. \tag{1}$$

Here, m (M) is the ion (atom) mass, and E_r is the radial part of the ion energy after the collision where we assume that the initial energy is solely in the axial direction. In Langevin collisions, $\cos(\theta)$, where θ is the scattering angle in the center-of-mass frame, is distributed isotropically (red lines in Fig. 3). However, our experimental limitations, which are mainly due to the binning of the radial energy due to the LRT mode analysis [31], result in a modified distribution indicated by the blue x's and gray shaded area in Fig. 3.

The experimental results of the data in Figs. 2(a)–2(d) are given in blue circles. We use the LRT to omit the no-collision events from the analysis; however, more-than-one-collision events are included, and we estimate them to consist of a total of 40% of the data [31]. Similar results are obtained using the data of Figs. 2(a)–2(c) which consist of only 25% of more-than-one-collision data.

Figure 3 shows a good agreement between the experimental and theoretical scattering angles for small angles $[0 < \cos(\theta) < 1]$; however, it deviates from theory in the forward-scattering $[\cos(\theta) \approx 1]$ and backward-scattering $[\cos(\theta) < 0]$ regimes. The forward-scattering deviation is due to glancing collisions which are not part of the Langevin model. The backward-scattering deviation is due to the collision large angle and small resulting ion's energy in the lab frame, both of which are not compatible with our LRT analysis.

In a second experiment, we initialize the ion in an oscillatory state along one of the trap radial modes and displace the atoms 20 μm away from the trap center [Fig. 1(a)] such that collisions occur in regions of high-amplitude oscillating electric fields. These fields can couple to the ion's kinetic energy during a collision which leads to heating even when colliding with essentially a zero-temperature atom [21–25].

The experimental results are shown in Figs. 4(a)–4(e). The ion's initial energy is 218.2 ± 8.8 K along the trap x-radial mode [green in Fig. 4(a)]. As we overlap the ion and atoms, the SSDCT identifies single collision events [red in Figs. 4(a)–4(e)] by the LRT method described above. In this experiment, we compare the experimental results to three numerical simulations, x-mode (green), z-mode (blue), and steady-state mode (red) distributions [Fig. 4(X)] and to MD simulations that have the same percentage of no-collision events at a given time. We see that before interaction, the LRT identified 99% of the events as x-mode events (green). This gives a bound for the

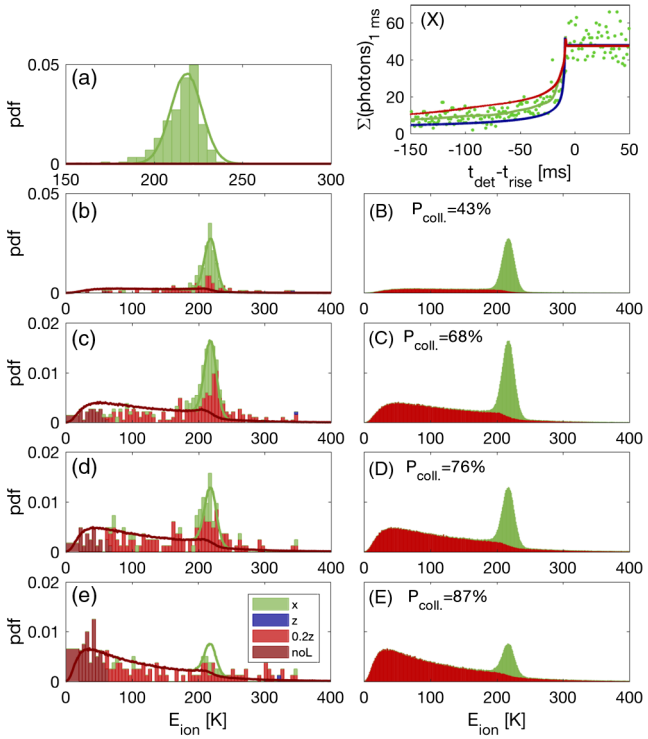

FIG. 4. Nonequilibrium dynamics. (X) Dots are the measured single-shot fluorescence signal where the ion's energy is initialized in the trap's x-radial mode. Lines are numerical calculation results where the ion's energy is initialized in the x mode (green), z mode (blue), and the steady-state mixture (0.4, x; 0.45, y; 0.15, z) of modes. (a)–(e) Experimentally measured total-energy histograms for increasing interaction time. The color of the bars indicates the result of the LRT, and it is the same as in (X). Dark red bars are low-energy events which are below the LRT sensitivity. The energy value of all events is extracted using the x-mode numerical calculation. Lines are MD-simulation results. The area underneath the red line represents events with at least a single collision while the area above the red line signals events which did not collide according to the simulation. (A)–(E) MD-simulation total-energy histograms. Color code indicates events which are more than 99% x mode (green) or z mode (blue). The rest of the events are colored in red. Probability for collision is given for each graph.

false collision detection error below 1%. We also see that the LRT identified events which collided with the atoms to be almost exclusively in the steady-state mode with agreement with the MD simulation [Figs. 4(B)–4(E)]. These events [marked in red in Figs. 4(b)–4(e)] can take values up to 350 K which are considerably larger than the ion's initial energy. We use the x-mode trajectory for extracting the energy of all events including the z-mode and the steady-state mode events. This way, we make sure that we are not overestimating the energy as in the previous axial experiment. Thus, here we show a direct observation of the nonequilibrium dynamics in atom-ion collisions. The nonequilibrium dynamics we observe in the experiment is more pronounced than what is predicted by the MD simulation. We believe this is due to a non-Gaussian profile of the

atomic cloud which leads to collisions in trap regions of even larger amplitude oscillating fields.

As in the previous experiment, we see a peak of collision events with the same energy as the initial energy of the ion. These forward-scattering (glancing) events are not accounted for in the MD simulation since it includes only Langevin (spiraling) collisions. This result together with the scattering angle analysis given in Fig. 3 emphasizes the sensitivity to collision directionality of the LRT and the ability to explore collision dynamics beyond the Langevin model.

To summarize, we used a novel thermometry technique (SSDCT) with single-event and energy-mode resolution to study the sympathetic cooling dynamics of an energetic ion immersed in an ultracold bath of neutral atoms. We demonstrated the capabilities of SSDCT to detect a single collision and the direction of ion motion following this collision. We used this capability to observe a deviation of the scattering angle distribution from the Langevin model predictions manifested by a forward-scattering peak. We also directly observed the nonequilibrium dynamics of atom-ion collisions in a Paul trap with single-collision resolution. Nonequilibrium dynamics and the resulting power-law distributions are considered as a hallmark of complex-systems dynamics. Ultracold atom-ion mixtures serve as a controllable test bed for the study and simulation of such nonequilibrium dynamics. Here, we presented the first experimental study of the emergence of these nonequilibrium effects, collision by collision. The tools we developed here will lead to better control and understanding of this complex dynamics.

We thank Eric Hudson and Ian Rouse for useful discussions. This work was supported by the Crown Photonics Center, ICore-Israeli excellence center circle of light, the Israeli Science Foundation, and the European Research Council (consolidator Grant No. 616919-Ionology).

*Present address: Department of Chemistry, University of Basel, Basel 4056, Switzerland.
ziv.meir@unibas.ch

[1] D. J. Larson, J. C. Bergquist, J. J. Bollinger, W. M. Itano, and D. J. Wineland, Sympathetic Cooling of Trapped Ions: A Laser-Cooled Two-Species Nonneutral Ion Plasma, Phys. Rev. Lett. **57**, 70 (1986).

[2] K. Mølhave and M. Drewsen, Formation of translationally cold MgH+ and MgD+ molecules in an ion trap, Phys. Rev. A **62**, 011401 (2000).

[3] P. Blythe, B. Roth, U. Fröhlich, H. Wenz, and S. Schiller, Production of Ultracold Trapped Molecular Hydrogen Ions, Phys. Rev. Lett. **95**, 183002 (2005).

[4] X. Tong, A. H. Winney, and S. Willitsch, Sympathetic Cooling of Molecular Ions in Selected Rotational and Vibrational States Produced by Threshold Photoionization, Phys. Rev. Lett. **105**, 143001 (2010).

[5] C. W. Chou, D. B. Hume, J. C. J. Koelemeij, D. J. Wineland, and T. Rosenband, Frequency Comparison of Two High-Accuracy Al+ Optical Clocks, Phys. Rev. Lett. **104**, 070802 (2010).

[6] S. Schiller and V. Korobov, Tests of time independence of the electron and nuclear masses with ultracold molecules, Phys. Rev. A **71**, 032505 (2005).

[7] T. Rosenband, D. B. Hume, P. O. Schmidt, C. W. Chou, A. Brusch, L. Lorini, W. H. Oskay, R. E. Drullinger, T. M. Fortier, J. E. Stalnaker, S. A. Diddams, W. C. Swann, N. R. Newbury, W. M. Itano, D. J. Wineland, and J. C. Bergquist, Frequency ratio of Al+ and Hg+ single-ion optical clocks; Metrology at the 17th decimal place, Science **319**, 1808 (2008).

[8] L. Ratschbacher, C. Zipkes, C. Sias, and M. Köhl, Controlling chemical reactions of a single particle, Nat. Phys. **8**, 649 (2012).

[9] T. Sikorsky, Z. Meir, R. Ben-shlomi, N. Akerman, and R. Ozeri, Spin controlled atom-ion inelastic collisions, Nat. Commun. **9**, 920 (2018).

[10] H. Fürst, T. Feldker, N. V. Ewald, J. Joger, M. Tomza, and R. Gerritsma, Dynamics of a single ion spin impurity in a spin-polarized atomic bath, arXiv:1712.07873 [Phys. Rev. A (to be published)].

[11] C. J. Myatt, E. A. Burt, R. W. Ghrist, E. A. Cornell, and C. E. Wieman, Production of Two Overlapping Bose-Einstein Condensates by Sympathetic Cooling, Phys. Rev. Lett. **78**, 586 (1997).

[12] A. G. Truscott, Observation of Fermi pressure in a gas of trapped atoms, Science **291**, 2570 (2001).

[13] A. Jöckel, A. Faber, T. Kampschulte, M. Korppi, M. T. Rakher, and P. Treutlein, Sympathetic cooling of a membrane oscillator in a hybrid mechanicalatomic system, Nat. Nanotechnol. **10**, 55 (2015).

[14] C. Zipkes, S. Palzer, C. Sias, and M. Köhl, A trapped single ion inside a Bose-Einstein condensate. Nature (London) **464**, 388 (2010).

[15] S. Schmid, A. Härter, and J. H. Denschlag, Dynamics of a Cold Trapped Ion in a Bose-Einstein Condensate, Phys. Rev. Lett. **105**, 133202 (2010).

[16] W. G. Rellergert, S. T. Sullivan, S. J. Schowalter, S. Kotochigova, K. Chen, and E. R. Hudson, Evidence for sympathetic vibrational cooling of translationally cold molecules, Nature (London) **495**, 490 (2013).

[17] S. J. Schowalter, A. J. Dunning, K. Chen, P. Puri, C. Schneider, and E. R. Hudson, Blue-sky bifurcation of ion energies and the limits of neutral-gas sympathetic cooling of trapped ions, Nat. Commun. **7**, 12448 (2016).

[18] Z. Meir, T. Sikorsky, R. Ben-shlomi, N. Akerman, Y. Dallal, and R. Ozeri, Dynamics of a Ground-State Cooled Ion Colliding with Ultracold Atoms, Phys. Rev. Lett. **117**, 243401 (2016).

[19] W. Paul, Electromagnetic traps for charged and neutral particles, Rev. Mod. Phys. **62**, 531 (1990).

[20] F. G. Major and H. G. Dehmelt, Exchange-collision technique for the rf spectroscopy of stored ions, Phys. Rev. **170**, 91 (1968).

[21] R. G. DeVoe, Power-Law Distributions for a Trapped Ion Interacting with a Classical Buffer Gas, Phys. Rev. Lett. **102**, 063001 (2009).

[22] C. Zipkes, L. Ratschbacher, C. Sias, and M. Köhl, Kinetics of a single trapped ion in an ultracold buffer gas, New J. Phys. **13**, 053020 (2011).

[23] K. Chen, S. T. Sullivan, and E. R. Hudson, Neutral Gas Sympathetic Cooling of an Ion in a Paul Trap, Phys. Rev. Lett. **112**, 143009 (2014).
[24] B. Höltkemeier, P. Weckesser, H. López-Carrera, and M. Weidemüller, Buffer-Gas Cooling of a Single Ion in a Multipole Radio Frequency Trap Beyond the Critical Mass Ratio, Phys. Rev. Lett. **116**, 233003 (2016).
[25] I. Rouse and S. Willitsch, Superstatistical Energy Distributions of an Ion in an Ultracold Buffer Gas, Phys. Rev. Lett. **118**, 143401 (2017).
[26] Z. Meir, T. Sikorsky, R. Ben-shlomi, N. Akerman, M. Pinkas, Y. Dallal, and R. Ozeri, Experimental apparatus for overlapping a ground-state cooled ion with ultracold atoms, J. Mod. Opt. **65**, 501 (2018).
[27] Z. Meir, T. Sikorsky, N. Akerman, R. Ben-shlomi, M. Pinkas, and R. Ozeri, Single-shot energy measurement of a single atom and the direct reconstruction of its energy distribution, Phys. Rev. A **96**, 020701 (2017).
[28] J. H. Wesenberg, R. J. Epstein, D. Leibfried, R. B. Blakestad, J. Britton, J. P. Home, W. M. Itano, J. D. Jost, E. Knill, C. Langer, R. Ozeri, S. Seidelin, and D. J. Wineland, Fluorescence during Doppler cooling of a single trapped atom, Phys. Rev. A **76**, 053416 (2007).
[29] T. Sikorsky, Z. Meir, N. Akerman, R. Ben-shlomi, and R. Ozeri, Doppler cooling thermometry of a multilevel ion in the presence of micromotion, Phys. Rev. A **96**, 012519 (2017).
[30] S. Dutta, R. Sawant, and S. A. Rangwala, Collisional Cooling of Light Ions by Cotrapped Heavy Atoms, Phys. Rev. Lett. **118**, 113401 (2017).
[31] See Supplemental Material at http://link.aps.org/supplemental/10.1103/PhysRevLett.121.053402 for details regarding experimental details, likelihood ratio test, stochastic simulation, and scattering angle calculation.
[32] J. I. Cirac, L. J. Garay, R. Blatt, A. S. Parkins, and P. Zoller, Laser cooling of trapped ions: The influence of micromotion, Phys. Rev. A **49**, 421 (1994).